D5.1.24 Real-time simulation results of protection and network automation options to improve the stability of DG unit in supplying feeder fault

Ontrei Raipala, Tampere University of Technology

Introduction

The amount of distributed generation (DG) connected to distribution networks keeps growing. More challenges related network protection are expected when several sources are feeding the distribution system. Problems related protection blinding, nuisance tripping of intelligent electric devices (IEDs), failed reclosing, unintentional islanding and fault ride through (FRT) requirements are the main problems related to the protection challenges related to the integration of DG. A novel protection automation system designed for overcoming these challenges was set up at Tampere University of Technology and hardware-in-loop real time simulations were performed in order to study the performance of the established protection system.

The studied protection automation system was also designed to increase the reliability of distribution service to DG units. This kind of service may be attractive to the owners of large DG units that are connected to remote locations, since even short outages may be harmful to them. The idea behind the proposed protection automation configuration is that distribution networks are often built meshed but operated in radial mode. In many cases a customer may have two or more line routes through which the supply is provided. The automation of distribution network is mainly limited currently to remotely controlled disconnectors and reclosers. Remotely controlled disconnectors are utilized to speed up the distribution network restoration process e.g. by providing a new supply behind a permanent fault via a backup connection. Reclosers are utilized to separate faulted part of network automatically i.e. they are utilized to reduce the interruption area.

The aim of the first case was to study how protection automation could aid in providing more reliable feeding path to DG units. The IEDs were configured to try to automatically change feeding path of the DG unit to another feeder in case of a fault in the original feeding path. In the second studied case, it was examined how voltage dips caused by faults on adjacent feeders may cause nuisance tripping of DG units. Additionally, a solution for avoiding nuisance tripping is demonstrated. A synchronous generator model was used in the first two studied cases. However, in the third case the synchronous generator was replaced by an induction generator and the studies of the first case were repeated. The principles behind the studied protection automation have been covered in [1] and [2].

Studied automation system

Automatic operation of remotely controlled disconnectors may improve the reliability of network at DG unit connection point remarkably. This can be illustrated by examining Fig. 1. A DG unit, which is situated at the tail part of feeder A, normally supplies power through feeder A which is protected with differential

protection scheme (Feeder IED A1 and A2). IED A2 is set to control both disconnector D_A and the normally open disconnector D_B. Thus, in case if a fault occurs on feeder A, IED A2 can switch the feeding route of the DG unit to feeder B automatically. The disconnectors were assumed to be able to break a maximum current of 630A which is in line with the breaking capacities of the commercial switch-disconnectors in references [3] and [4].

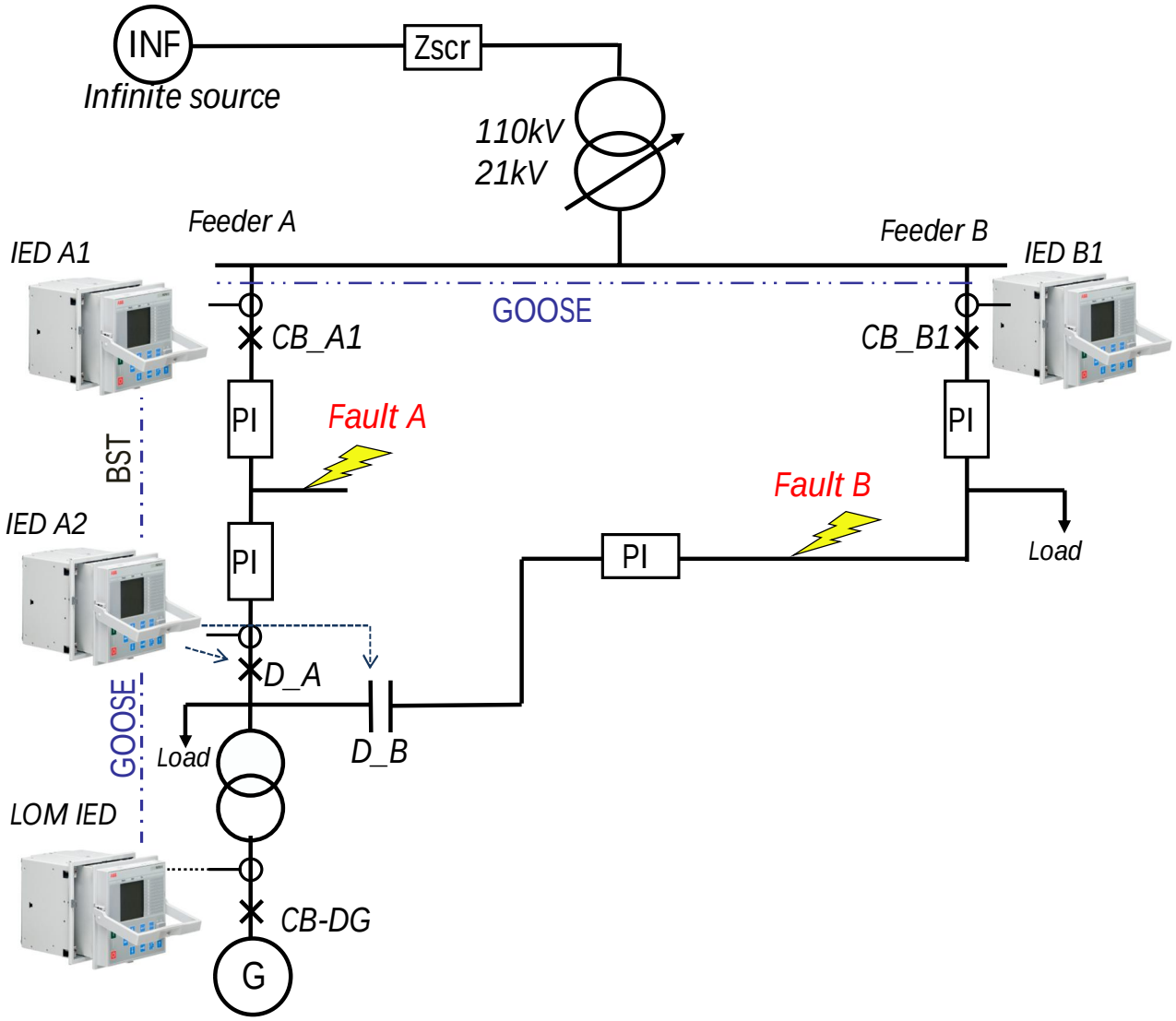

Fig. 1. The network model used in radial network configuration studies

When a fault occurs at fault location A in Fig. 1, the differential protection isolates this fault by opening circuit breaker A1 and disconnector D_A. IED A2 then immediately sends a trip command to DG IED since unintentional islanding is prohibited and because the fault current fed by the DG unit may sustain the fault arc between the contacts of disconnector D_A. After this, IED A2 sends a close command to the normally open disconnector D_B and after a chosen delay, a close permit to DG IED. However, the actual closing time of the DG unit circuit breaker is decided by the synchronism check function (SECRSYN) in the DG IED.

The synchronism check settings used in these studies are based on [5] – [7]. These and other IED settings are visible at the end of this document in the "IED settings" chapter.

While planning the delays between the various switching, the following things were kept in mind.

- The combined time needed for the opening of a circuit breaker and the extinguishment of the fault arc between the circuit breaker contacts is approximately 100ms.
- The closing time of circuit breaker is in the range of 30-50ms [8]
- The fault current from the DG unit may delay the extinguishment of the fault arc in disconnector D_A. The fault arc is likely to extinguish shortly after the tripping of CB_DG. The time required for the opening of a circuit breaker and the extinguishment of the fault arc should happen within 100ms after the trip command from the respective IED.
- A trip command to CB_DG is given via GOOSE in approximately 3ms after the tripping of the differential relays. Disconnector D_B should not be closed before the extinguishment of the fault arc in disconnector D_A.
- Thus, in these studies it is assumed that a delay time of minimum 100ms (50ms delay for trip command + 100ms for CB opening and fault extinguishment – 50ms closing delay of D_B = 100ms) should exist between the trip command to CB_DG and close command to D_B.

Simulation hardware setup

The simulator

The simulation studies presented here were conducted using the real time digital simulator (RTDS). RTDS was chosen for these studies since it provides very accurate real time electromagnetic transient simulation for power systems and enables hardware-in-the-loop simulations. The current and voltage signals from chosen network nodes were fed as analogue output signals from the RTDS to two Omicron CMS156 amplifiers, which amplified the signals to proper scale for the IEDs. The IEDs then sent their control decisions concerning the circuit breakers and disconnectors back to the RTDS as digital signals via copper wires. More information regarding the simulation environment can be found from references [9] and [10].

Utilized IEDs

Modern IEDs utilizing inter-IED communication were chosen for these studies. The two differential IEDs, that is, A1 and A2, were of ABB RED615 type. These IED types are beneficial in the sense that the optical link between the IEDs can be used to transfer 7 user definable bits, as for instance trip and block commands. Thus, the communication between the IEDs is not limited to horizontal communication but also vertical communication is possible. Horizontal communication between the IEDs is accomplished with the help of IEC61850 GOOSE messages. The LOM IED at the end of feeder A and the overcurrent IED at the beginning of feeder B were of ABB REF615 type. A summary of the utilized settings in the IEDs is shown in table I. A more detailed description of the IED settings is given the appendix A.

Table I. Summary of the utilized protection settings

Line differential prot.		**Synchronism check settings**	
function	limit	function	limit
High op. val.	2000 %In	Δ V	0.08xUn
Low op. val.	10 %In	Δ f	0.5 Hz
End sect. 1	100 %In	Δ angle	10 deg
Slope sect. 2	50%	Energizing time	100 ms
End sect. 2	500 %In	Closing time of CB	40 ms
Slope sect. 3	150%	Live dead mode	Live Line, Dead Bus
Operate delay	45 ms		
I_nominal	100 A	**Loss of mains protection**	
		function	limit / delay
		UV	0.5 p.u. / 150 ms
Overcurrent prot. (B1)		OV	1.15 p.u. / 150 ms
function	limit	OFP	51 Hz / 200 ms
Start value	250 A	UFP	48 Hz / 200 ms
Operate delay	150 ms	ROCOF	2 Hz/s / 400 ms

The simulation models

Network model

The simulations were performed in a simple overhead line medium voltage network which is shown in Fig. 1. Two feeders, of which one is strong and the other is weak were connected to the substation. The positive sequence resistances and reactances of the PI line sections used for modelling the feeders are shown in table II. The loads were modelled as constant current loads. The values for the load on feeder A were 0.49MW and 0.14MVar and respectfully 0.31MW and 0.09MVar for feeder B.

Table II. The resistances and reactances of the PI sections used for modelling the feeders

From	To	R+	X+
Substation	Fault point A	1.215202	1.2350156
Fault point A	Feeder A end	4.860808	4.9400624
Substation	Fault point B	2.6636035	1.2963857
Fault point B	Feeder B end	23.9724315	11.6674713

Synchronous generator model

In the following, real time simulation studies were conducted using a directly coupled 1.6MVA rated hydro power driven synchronous generator (SG). This DG unit was connected to the tail part of feeder A via a 0.66kV/21kV step up transformer as shown in Fig. 1. The reactive power control of the synchronous generator model was realized using a cascade control, where a control loop determined the set point of the automatic voltage regulator with the aim of maintaining the reactive power output at a target value. Certain simplifications, namely the omission of the turbine controller modeling and the assumption of constant torque were made in the models. These measures are justified since hydro power plants have relatively high inertial mass which makes them respond to changes slowly, whereas, LOM protection studies are dealing with short timeframes only. The omission of turbine controller is justified because DG units are typically not attending to frequency control. More information regarding this DG unit model can be found from [9]. The generator was operated at unity power factor throughout the studies.

Induction generator model

The 1.8MVA rated induction generator utilized in the studies is modelled based on [11]. A shunt capacitor was connected to the generator side of the CB_DG switch in parallel with the DG unit. The value of the capacitor was chosen so that the power factor of the generator was approximately 0.98. The reasoning behind this value is that full compensation is usually not desired in order to avoid the self-excitation problem related to induction generators.

Simulation results

Switching the supplying route of a synchronous generator

In the first studied case, the aim was to examine if the synchronous generator would maintain its stability through the switching sequence. In order for the feeding path change of the DG unit to be successful, however, the synchronism check requirements naturally also had to be fulfilled. Inertia constant of the generator usually has a significant effect on the stability of synchronous generators, and therefore, three different inertia constant values were used for the generator. Additionally, it is evident that the mechanical torque driving the generator also has a significant impact on the stability of the generator when the electrical counter torque is null. The results from the studies are shown in table III.

Table III. The captured operation times of the circuit breakers in SG 1600MVA case

H [s]	Tm [p.u.]	t_CB_A1 [s]	t_CB_A2 [s]	t_B2_close [s]	t_DG_close [s]
1	0.45	0.143	0.1436	0.2429	failed
1	0.44	0.1432	0.1441	0.2451	0.5232
1	0.43	0.1423	0.144	0.2418	0.4976
2	0.44	0.1439	0.1419	0.2456	failed
2	0.43	0.1448	0.142	0.2462	0.5039
3	0.43	0.1453	0.145	0.2477	failed
3	0.42	0.1436	0.1454	0.2481	0.5048

The circuit breaker switching times in table III are in seconds from the beginning of the fault and they include the mechanical delays as well as the fault arc extinguishment delays. It can be seen from the table that the increment of the inertia constant value has a surprisingly minor effect on the studied fault ride through capability of the DG unit.

A selection of chosen graphs from one of the simulated cases (H=2s, Tm=0.43pu) presented in table III is shown in Fig. 2. In this case the DG unit maintained its stability while the protection automation system switched the DG unit feeding path to another feeder. The topmost graph in Fig. 2 presents the speed of the generator (rad/s), the graph below this presents the frequency of the connection point voltage of the DG unit (Hz), the third graph presents the voltage magnitudes from both sides of the DG unit circuit breaker (in per unit scale), the fourth graph presents the circuit breaker statuses (0=open, 1=closed) and finally, the last graph presents the angle difference of the voltages between both sides of the DG unit circuit breaker. Note that in the fourth graph that the delays from the open/close pulses from IEDs to the switching of the circuit breakers and disconnectors are taken into account. The closing delay is assumed to be 50ms, whereas, the combined time delay needed for the extinguishment of the fault arc and the opening of a switch is assumed to be 100ms.

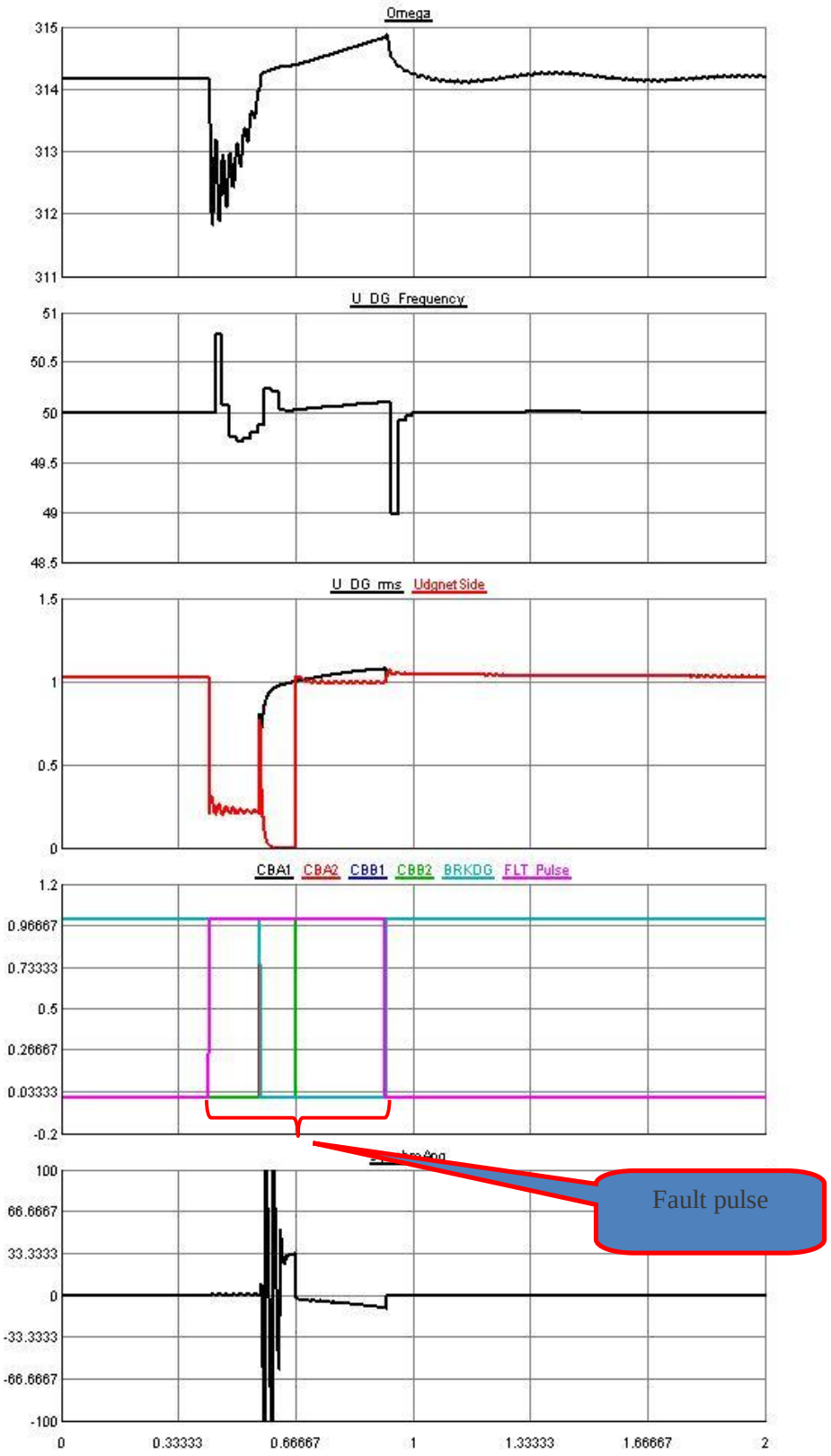

Fig. 2. Chosen graphs from the SG1600MVA, H=2, Tm0.43pu case presented in table III.

It can be seen from the lowest graph that it takes rather long for the synchronism check function to allow the reconnection of the generator. This most likely stems from the fact that the voltages on the other side of the DG unit circuit breaker drop to zero during the switching sequence and thus the IED is unable to obtain a frequency measurement until the voltages are restored. Moreover, it will still take some more time to get a reliable frequency measurement after the voltages are restored. Synchronism check function is therefore unable to ensure that the frequency difference between the two sides of the DG unit circuit breaker is within the specified limits (+-10deg.).

This problem can be alleviated to some extent by taking the voltage measurements from the end of feeder B instead of the other side of the DG unit circuit breaker. This is based on the fact that the voltages at the end of feeder B do not drop to zero and the frequency measurement is therefore not lost. By doing this, the reconnection time of the synchronous generator can be reduced approximately by 90ms in the case presented in Fig. 2. This reduction in the reconnection time of the DG unit also enabled the torque of the generator to be increased to 0.45pu without causing stability problems to the generator. It is noteworthy that the phase shifting effect of the DG transformer has to be taken into account when this approach is chosen. This can be done by setting -30deg to the “phase shift” setting of the SECRSYN function. Naturally, a different voltage transformer is also required if the other voltage is measured from the MV side (in RSCAD this was done by changing the scaling factor from 0.953 to 30.15 in the GTAO component).

Note that the functioning of the transfer trip based LOM protection is not highlighted here. However, as it can be seen from Fig. 2, the delay for the trip signal from differential IED A2 to the LOM IED takes less than 5ms. This feature is presented more in detail in references [1] and [2].

Avoidance of nuisance tripping

Faults on parallel feeders may cause so deep voltage dips in the connection point of the DG units that the undervoltage protection of DG relay unintentionally trips the DG unit. A situation of this kind is simulated in the following. A fault at the beginning of feeder B occurs and the responsible feeder protection trips the feeder off for a reclosing period of 300ms. This, however, causes a voltage dip also in the parallel feeders and the DG relay trips the DG unit unintentionally as shown in Fig. 3. The topmost graph in Fig. 3 presents the connection point voltages of the generator, the graph below this presents the voltage magnitudes from both sides of the DG unit circuit breaker, the third graph presents the circuit breaker statuses (0=open, 1=closed) and finally, the last graph presents the currents flowing through the circuit breaker at the beginning of feeder B (CB_B1).

The nuisance tripping problem can be avoided with the help of inter-IED communication. This was demonstrated by configuring IED B1 to send a block command to the LOM IED via IED_A1 and IED_A2 whenever IED B1 noticed a fault in its protection area. The messages between IED B1 and IED A1 are transmitted with the help of GOOSE messages, whereas, the messages between IED A1 and IED A2 is accomplished with the help of binary signal transfer (through the optical link).

A case like this was simulated and the same selection of graphs was chosen to be included in Fig 4. It can be seen from the graphs that the connection point voltage of the DG unit dips similarly as in the case where no communication was included. However, this time the block command prevents the unwanted disconnection of the DG unit.

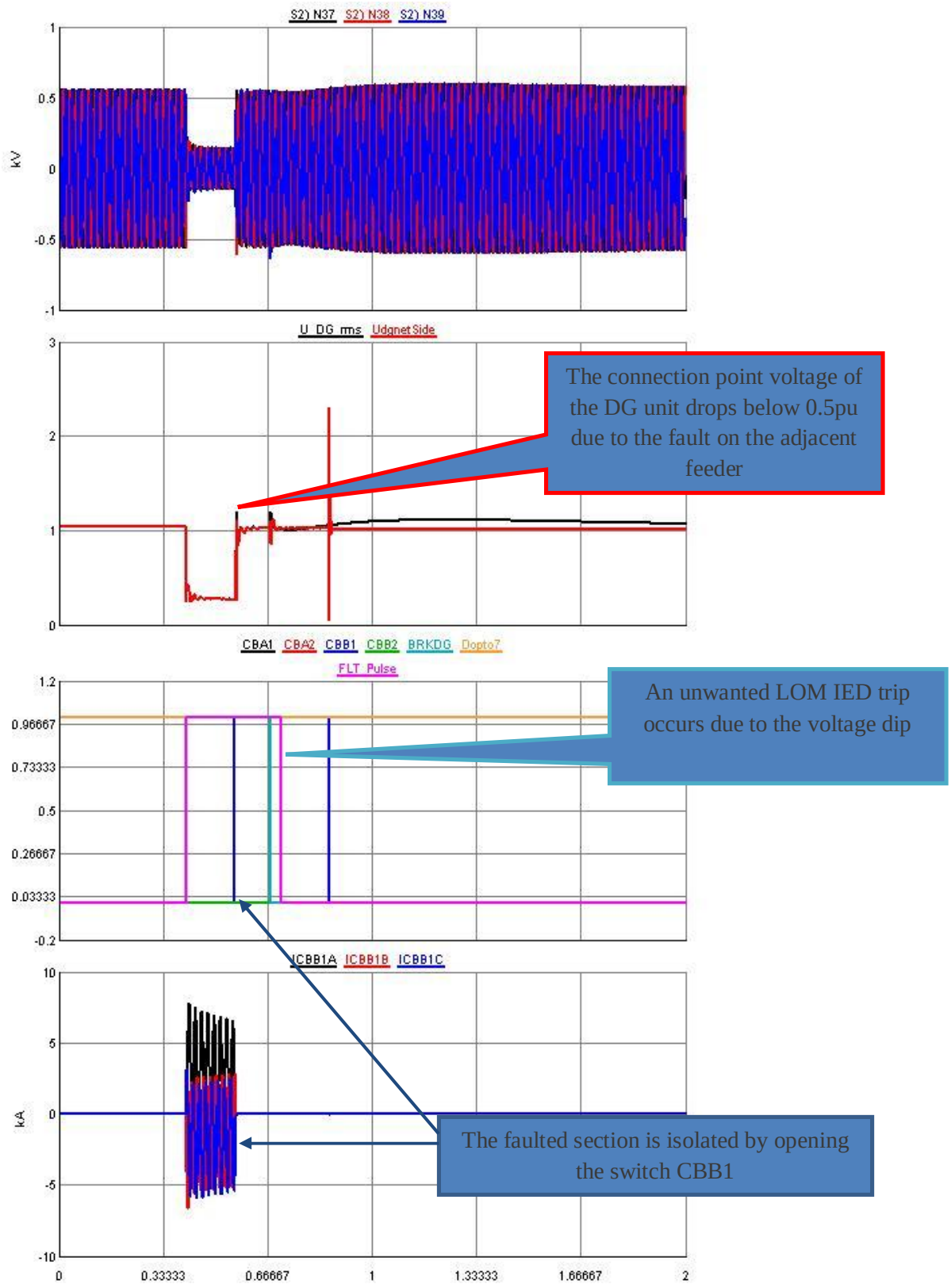

Fig 3. No inter-IED communication, a three phase short circuit in the beginning of feeder B

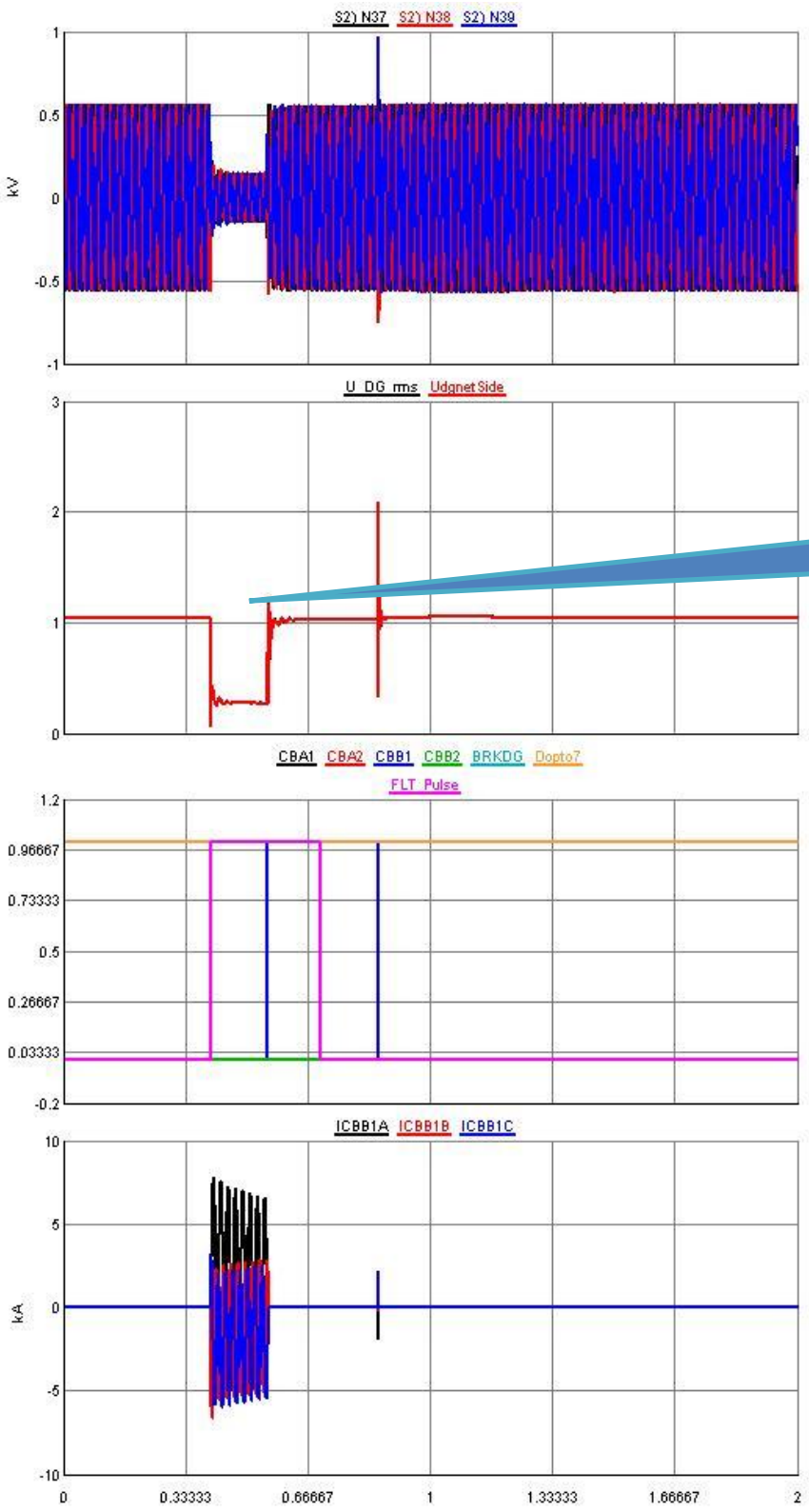

Fig. 4. With inter-IED communication, a three phase short circuit in the beginning of feeder B, a block command from IED03 blocks the UV protection of the DG relay.

Induction generator related studies

The synchronization requirements for small generators which were used in these studies allow an unsynchronized connection of an asynchronous generator when the slip difference is within specified limits as follows [1-3]:

$$\Delta n \leq \pm 5\% \, n_N \quad (1)$$

Because of this special loosened requirement for asynchronous generators, the settings of the SECRSYN function were loosened as well in order to better allow the reconnection of the generator after the switching sequence. The requirement (1) was manually checked afterwards by checking that the speed of the generator did not exceed the value 1.05*2*π*50=329.8 [rad/s].

The simulations were performed using the same network model as in the previous studies. The utilized DG unit was the 1.8MVA rated wind turbine driven asynchronous generator. A shunt compensation capacitor with a value of 2920µF was connected in parallel with the DG unit at the generator side of the CB_DG. Thus, the power factor of the DG unit was approximately 0.98 inductive.

Fig. 5 shows a selection of chosen graphs from the asynchronous generator case. The topmost graph presents the speed of the generator in radians per second scale, whereas, the second graph shows the connection point voltages of the DG unit. The third graph presents the connection point rms-voltages from both sides of the circuit breaker connecting the DG unit to the network. The fourth graph presents the statuses of the circuit breaker (0=open, 1=closed) and the duration of the fault pulse (0=no fault, 1=fault on). Finally, the last graph presents the currents flowing through the DG unit circuit breaker.

It can be seen from the second graph from the top of Fig. 5 that the voltages dip significantly during the fault. However, the voltages do not decay completely due to the presence of the shunt capacitor connected to the generator side of the CB_DG switch. It is also visible in the same graph that a considerable voltages dip is present after the reconnection of the generator (the reconnection moment is marked with a dashed line in the graphs). This is caused by the large magnetizing current taken by the induction generator. This voltage dip problem can be alleviated to some extent by utilizing an induction generator with a larger rotor resistance. However, a higher rotor resistance also causes more losses, which reduces the attractiveness of this manoeuvre. In the following, the rotor resistance was increased by 50%, that is, to 0.093p.u. and the previous simulation case was repeated. With this rotor resistance value, the speed of the generator barely managed to stay below the required limit as it can be seen from the top most graph of Fig. 6.

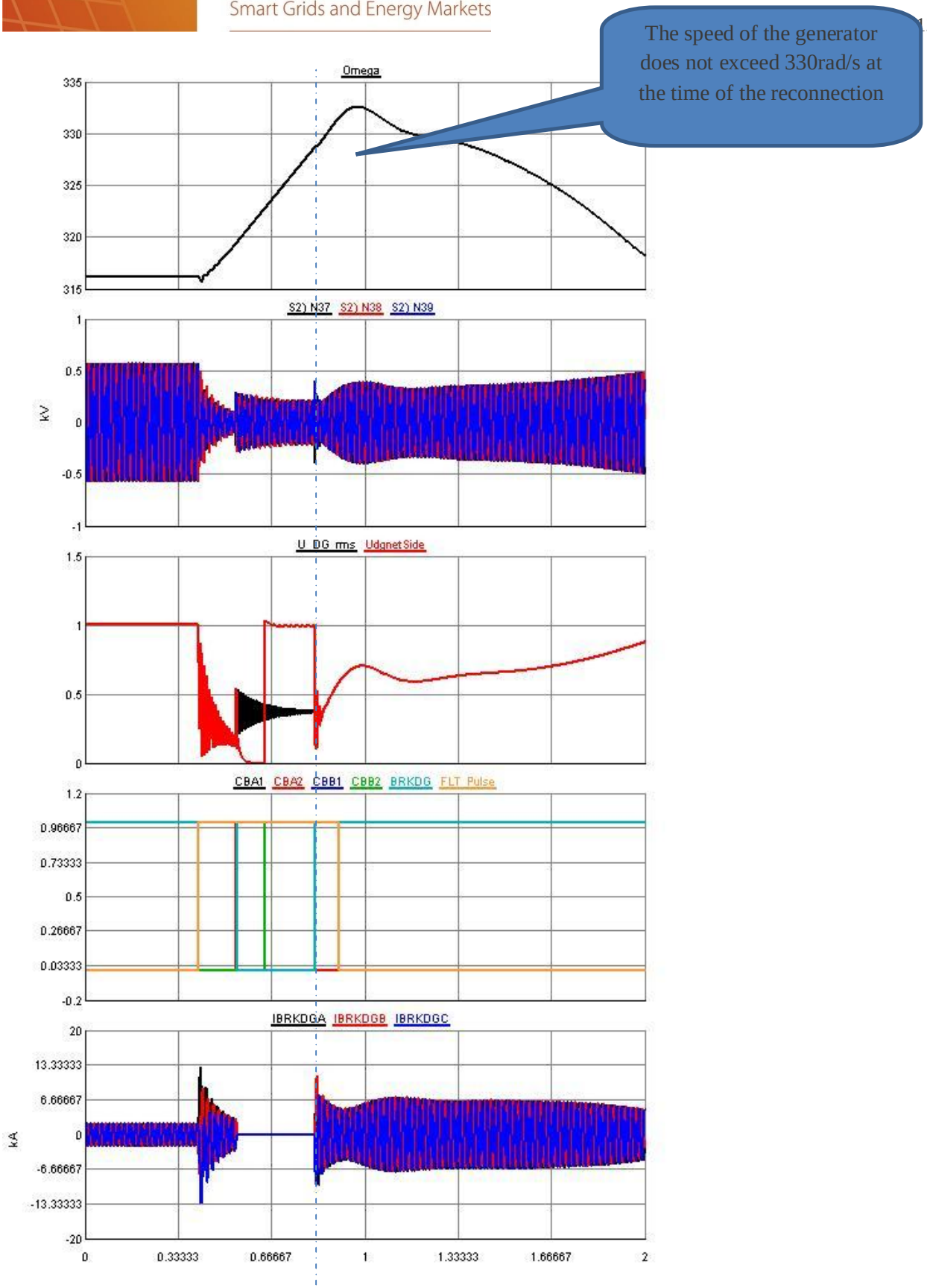

Fig. 5. 1.8MVA induction generator, original weak network, pf0.98ind, Rr=0.0062pu

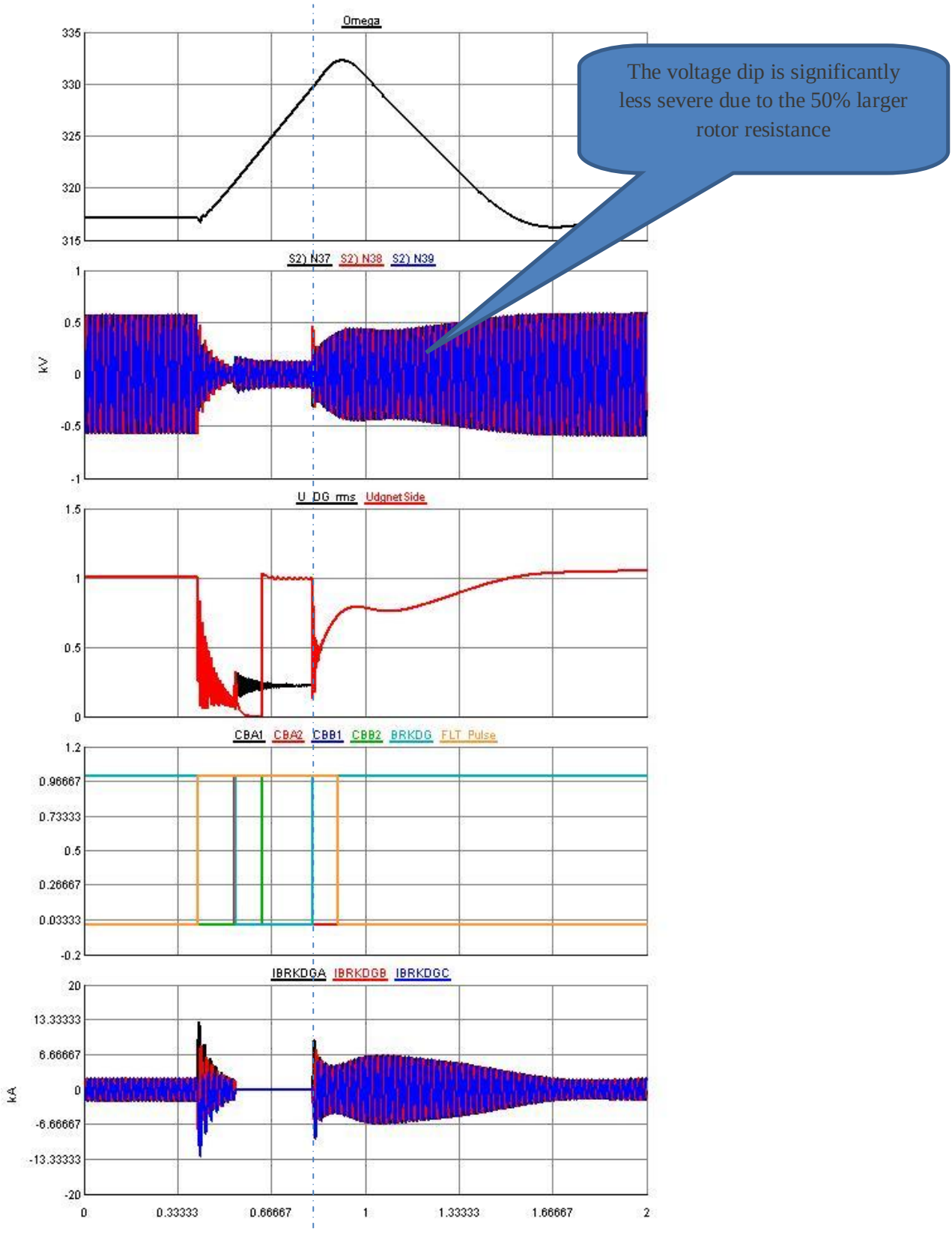

Fig. 6. 1.8MVA induction generator, original weak network, pf0.98ind, Rr=0.0093pu

Discussion

The studied communication based protection system provides a number of benefits for a distribution system which contains DG. The benefits are:

- Fast tripping of DG units during unintentional islanding and complete elimination of NDZ problem
- Avoidance of failed reclosing problem
- Avoidance of protection blinding problem
- Avoidance of nuisance tripping
- Full compatibility of LOM protection and FRT requirements

However, the reliability and speed of the communication medium are crucial. Speed of the communication is especially crucial in the case of the simulated feeding path switching and tripping of DG during fast autoreclosing. Despite the high performance of communication based protection schemes, reliable back up protection should always be available since communication failures may occur for instance due to human mistakes.

Special attention should be given to the coordination of the primary communication based protection and the local back up protection. It is of no help that a DG unit capable of riding through a fault if the local LOM IED controlling the DG unit circuit breaker is not set to allow the FRT. Local LOM protection thus has to be set to allow the FRT by loosening the LOM IED settings. This, however, degrades the performance of local LOM protection significantly [12].

The studied protection automation system is able to guarantee fail proof LOM protection and full FRT compatibility. This is accomplished by setting the local LOM protection to allow FRT when the communication based protection is functioning. Otherwise local LOM protection functions such undervoltage or rate of change of voltage may unwantedly trip the DG unit due to voltage dips caused by remote grid faults. Stricter local LOM protection should be activated only if a failure in the communication link is detected. However, in case if the activation of stricter local LOM protection is needed due to communication failure, it should be done rapidly and automatically since unintentional islanding raises safety risks not only to components but also human beings. It is noteworthy that the stricter local LOM protection settings should only be enabled in case if the communication between the relevant IEDs forming the vital part of the communication link to the LOM IED failed. For instance, there would be no need to activate stricter local LOM protection if the communication between IED B1 and IED A1 in Fig. 1 failed. FRT related issues were, nevertheless, not simulated in this study since the undervoltage protection settings of the LOM IED were set according to the requirements in references [5] – [7].

The downside of communication based protection systems is always the cost associated with establishing the required communication infrastructure. The studied protection system has the advantage that it utilizes the optical communication link between the differential IEDs and thereby requires no additional communication medium for vertical direction communication. The horizontal inter IED communication is established with standard GOOSE messages.

Conclusions

A novel protection automation system was established and its ability to solve protection challenges related to DG was studied. The system is utilizes IEC-61850 GOOSE messages for horizontal inter IED communication and the optical wire between differential IEDs for vertical inter IED communication. A hardware-in-the-loop simulation environment was used for testing the performance of the established system.

The purpose of the first studied case was to examine if the protection system would be able to increase the reliability of distribution service to DG units by automatically switching an alternative feeding path to the DG unit when the original feeding path is faulted. This was found to be true especially in asynchronous generators case where it was possible to switch the feeding path of the DG unit at nominal power. However, the service reliability enhancement was of minor scale in synchronous generators case since the feeding path switching was only possible with rather small values of mechanical torque.

In the second case it was studied how the protection system could prevent nuisance tripping of DG. The results clearly showed that nuisance tripping problem caused by faults on the adjacent feeders can be avoided with the help of the studied protection automation system. The proposed protection system is also able to provide rapid and fully fail proof LOM protection with full FRT compatibility.

Appendix A. IED settings

The utilized IED settings are visible in the following tables.

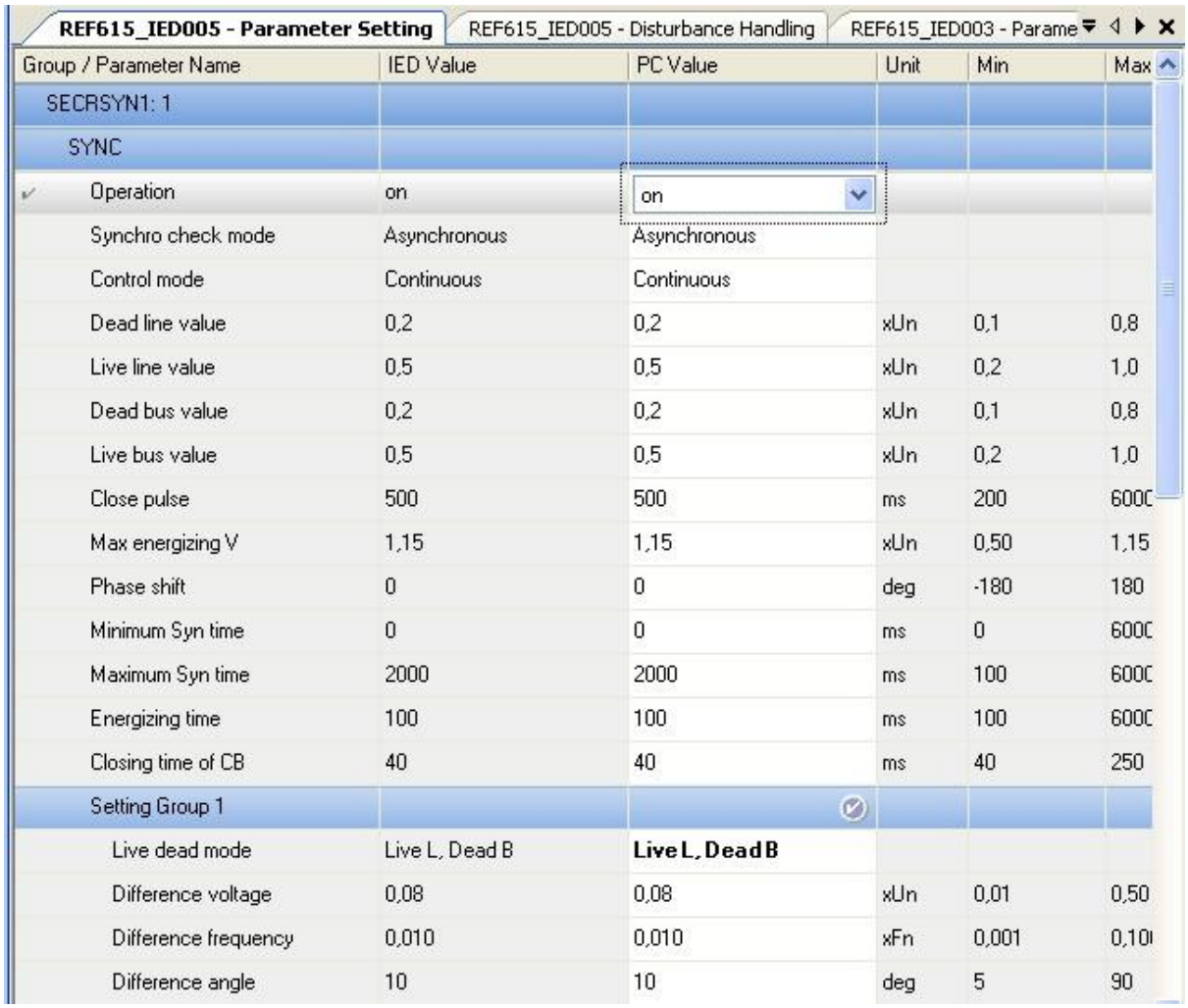

REF615_IED005 - Parameter Setting | REF615_IED005 - Disturbance Handling | REF615_IED003 - Parame

Group / Parameter Name	IED Value	PC Value	Unit	Min	Max
SECRSYN1: 1					
SYNC					
Operation	on	on			
Synchro check mode	Asynchronous	Asynchronous			
Control mode	Continuous	Continuous			
Dead line value	0,2	0,2	xUn	0,1	0,8
Live line value	0,5	0,5	xUn	0,2	1,0
Dead bus value	0,2	0,2	xUn	0,1	0,8
Live bus value	0,5	0,5	xUn	0,2	1,0
Close pulse	500	500	ms	200	600(
Max energizing V	1,15	1,15	xUn	0,50	1,15
Phase shift	0	0	deg	-180	180
Minimum Syn time	0	0	ms	0	600(
Maximum Syn time	2000	2000	ms	100	600(
Energizing time	100	100	ms	100	600(
Closing time of CB	40	40	ms	40	250
Setting Group 1					
Live dead mode	Live L, Dead B	**Live L, Dead B**			
Difference voltage	0,08	0,08	xUn	0,01	0,50
Difference frequency	0,010	0,010	xFn	0,001	0,10(
Difference angle	10	10	deg	5	90

Note that dead bus value significantly affects the synchronization capability of the DG unit as the SECRSYN function allows a dead bus to be connected to the energized line when the live dead mode is set to “Live L, Dead B”. In the induction generator case the dead bus value was increased to 0.5xUn because of the loosened connection requirements discussed in wind turbine case chapter.

REF615_IED005 - Parameter Setting | REF615_IED005 - Disturbance Handling | REF615_IED003 - Parame

Group / Parameter Name	IED Value	PC Value	Unit	Min	Max
Voltage (3U,VT): 1					
Voltage (3U,VT)					
Primary voltage	0,400	**0,400**	kV	0,100	440,000
Secondary voltage		100	V	60	210
VT connection	Wye	Wye			
Amplitude corr. A		1,000		0,900	1,100
Amplitude corr. B		1,000		0,900	1,100
Amplitude corr. C		1,000		0,900	1,100
Voltage input type		Voltage trafo			

REF615_IED005 - Parameter Setting | REF615_IED005 - Disturbance Handling | REF615_IED003 - Parame

Group / Parameter Name	IED Value	PC Value	Unit	Min	Max
Voltage (3UB,VT): 2					
Voltage (3UB,VT)					
Primary voltage	0,400	0,400	kV	0,100	440,000
Secondary voltage		100	V	60	210
VT connection		UL1			
Amplitude corr. A		1,000		0,900	1,100
Voltage input type		Voltage trafo			

Note that the setting “primary voltage” refers to the L-N voltage of the connection point. Two different values were thus utilized for these settings since nominal the L-N voltage of the synchronous generator was 0.381kV, whereas, for the induction generator case the respective value was 0.4kV. This naturally also had to be taken into account in the D/A output scaling of RTDS GTAO component.

REF615_IED005 - Parameter Setting | REF615_IED005 - Disturbance Handling | RED615_IED002 - Parameter

Group / Parameter Name	IED Value	PC Value	Unit	Min	Max
PHPTUV1: 1					
3U<(1)					
Operation	on	**on**			
Num of start phases		1 out of 3			
Minimum operate time	150	**150**	ms	60	60000
Reset delay time		20	ms	0	60000
Curve parameter A		1,000		0,005	200,000
Curve parameter B		1,00		0,50	100,00
Curve parameter C		0,0		0,0	1,0
Curve parameter D		0,000		0,000	60,000
Curve parameter E		1,000		0,000	3,000
Curve Sat Relative		2,0		0,0	3,0
Voltage block value		0,20	xUn	0,05	1,00
Enable block value		True			
Voltage selection		phase-to-phase			
Relative hysteresis		4,0	%	1,0	5,0
Setting Group 1					
Start value	0,50	**0,50**	xUn	0,05	1,20
Time multiplier		1,00		0,05	15,00
Operate delay time		100	ms	60	300000
Operating curve type		IEC Def. Time			
Type of reset curve		Immediate			

REF615_IED005 - Parameter Setting | REF615_IED005 - Disturbance Handling | RED615_IED002 - Parameter

Group / Parameter Name	IED Value	PC Value	Unit	Min	Max
PHPTOV1: 1					
3U>(1)					
Operation	on	**on**			
Num of start phases		1 out of 3			
Minimum operate time	150	**150**	ms	40	60000
Reset delay time		20	ms	0	60000
Curve parameter A		1,000		0,005	200,000
Curve parameter B		1,00		0,50	100,00
Curve parameter C		0,0		0,0	1,0
Curve parameter D		0,000		0,000	60,000
Curve parameter E		1,000		0,000	3,000
Curve Sat Relative		2,0		0,0	3,0
Voltage selection		phase-to-phase			
Relative hysteresis		4,0	%	1,0	5,0
Setting Group 1					
Start value	1,15	**1,15**	xUn	0,05	1,60
Time multiplier		1,00		0,05	15,00
Operate delay time		40	ms	40	300000
Operating curve type		IEC Def. Time			
Type of reset curve		Immediate			

Group / Parameter Name	IED Value	PC Value	Unit	Min	Max
FRPFRQ1: 1					
f>/f<,df/dt(1)					
Operation	on	on			
Reset delay Tm Freq	0	0	ms	0	6000
Reset delay Tm df/dt	0	0	ms	0	6000
Setting Group 1					
Operation mode	Freq<	Freq<			
Start value Freq>	1,020	1,020	xFn	0,900	1,20
Start value Freq<	0,960	0,960	xFn	0,800	1,10
Start value df/dt	0,040	0,040	xFn /s	-0,200	0,20
Operate Tm Freq	200	200	ms	80	200
Operate Tm df/dt	400	400	ms	120	200

Group / Parameter Name	IED Value	PC Value	Unit	Min	Max
LNPLDF1: 1					
3dI>L					
Operation	on	on			
Restraint mode	None	None			
Reset delay time	0	0	ms	0	6000
Minimum operate time	45	45	ms	45	6000
CT ratio correction	1,000	1,000		0,200	5,000
CT connection type	Type 1	Type 1			
Setting Group 1					
High operate value	2000	2000	%In	200	4000
High Op value Mult	1,0	1,0		0,5	1,0
Low operate value	10	10	%In	10	200
End section 1	100	100	%In	0	200
Slope section 2	50	50	%	10	50
End section 2	500	500	%In	200	2000
Slope section 3	150	150	%	100	200
Operate delay time	45	45	ms	45	2000
Operating curve type	IEC Def. Time	IEC Def. Time			
Time multiplier	1,00	1,00		0,05	15,00
Start value 2.H	20	20	%	10	50

ting | RED615_IED002 - Parameter Setting | REF615_IED004 - Parameter Setting | RED615_IED001 - Parame

Group / Parameter Name	IED Value	PC Value	Unit	Min	Max
LNPLDF1: 1					
3dI>L					
Operation	on	on			
Restraint mode	None	None			
Reset delay time	0	0	ms	0	600(
Minimum operate time	45	45	ms	45	600(
CT ratio correction	1,000	1,000		0,200	5,00
CT connection type	Type 1	Type 1			
Setting Group 1					
High operate value	2000	2000	%In	200	400(
High Op value Mult	1,0	1,0		0,5	1,0
Low operate value	10	10	%In	10	200
End section 1	100	100	%In	0	200
Slope section 2	50	50	%	10	50
End section 2	500	500	%In	200	200(
Slope section 3	150	150	%	100	200
Operate delay time	45	45	ms	45	200(
Operating curve type	IEC Def. Time	IEC Def. Time			
Time multiplier	1,00	1,00		0,05	15,0
Start value 2.H	20	20	%	10	50

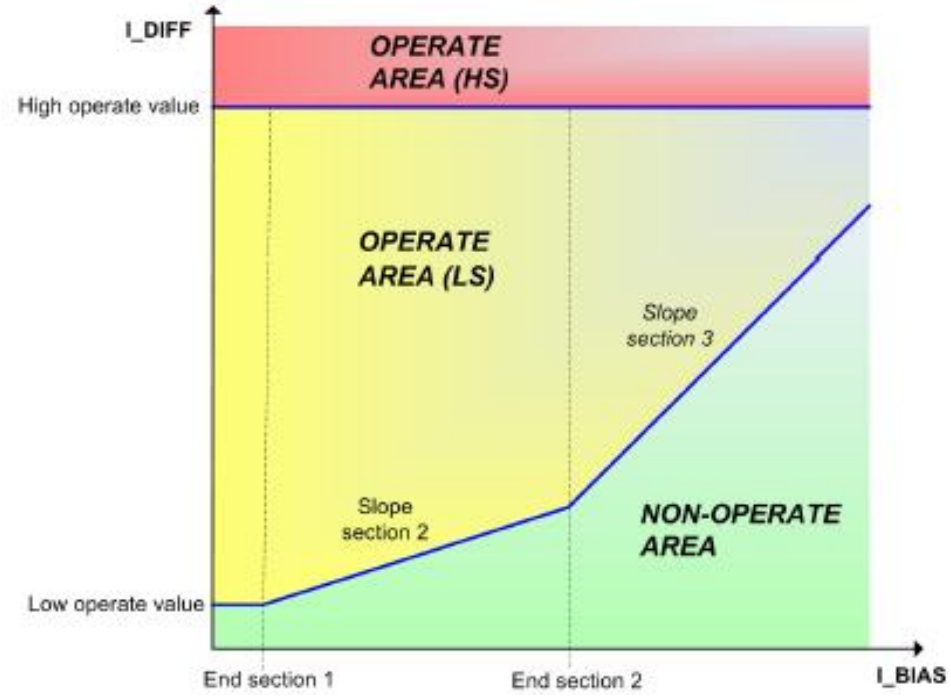

Fig 7. Operating principle of differential protection

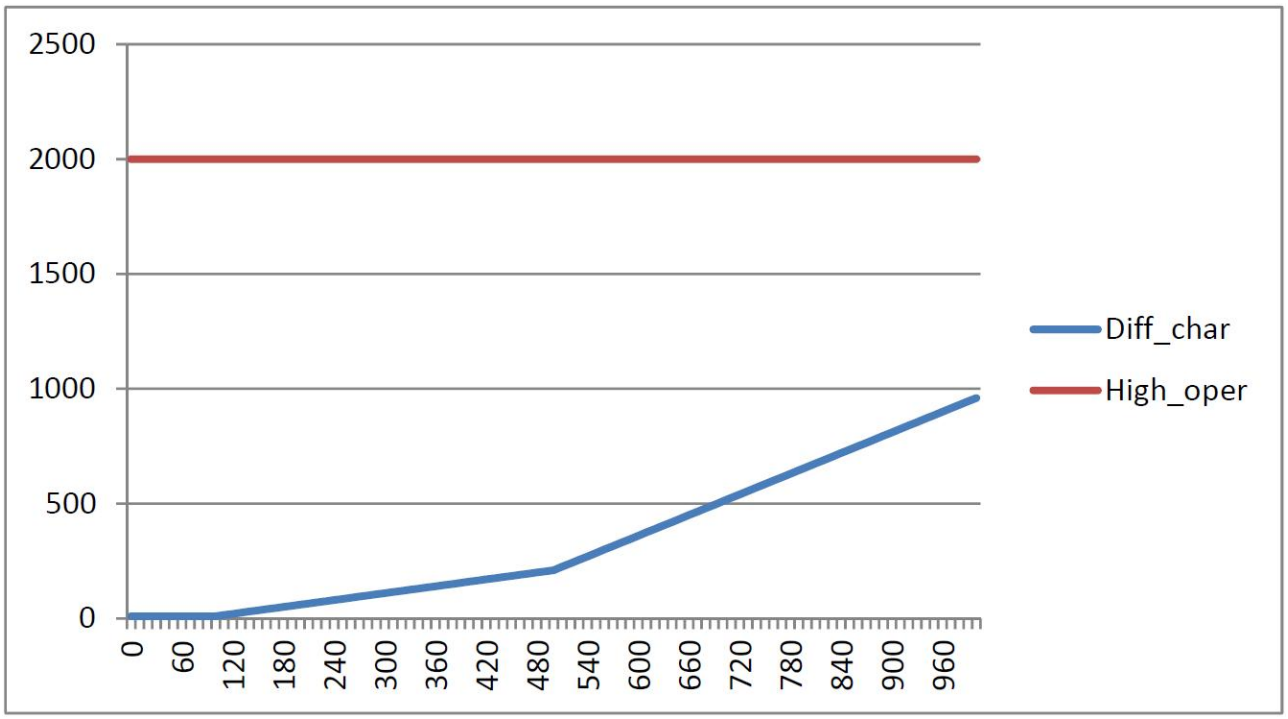

Fig. 8. Operating characteristics of the utilized differential protection function

Group / Parameter Name	IED Value	PC Value	Unit	Min	Max
DPHLPDOC1: 1					
3I>->(1)					
Operation	on	on			
Num of start phases	1 out of 3	1 out of 3			
Curve parameter A	28,2000	28,2000		0,0086	120,
Curve parameter B	0,1217	0,1217		0,0000	0,71
Curve parameter C	2,00	2,00		0,02	2,00
Curve parameter D	29,10	29,10		0,46	30,0
Curve parameter E	1,0	1,0		0,0	1,0
Allow Non Dir	False	False			
Setting Group 1					
Start value	2,50	2,50	xIn	0,05	5,00
Operate delay time	150	**150**	ms	40	200(
Operating curve type	IEC Def. Time	IEC Def. Time			
Voltage Mem time	40	40	ms	0	300(
Directional mode	Non-directional	Non-directional			
Characteristic angle	60	60	deg	-179	180
Pol quantity	Cross pol	Cross pol			

15_IED005 - Parameter Setting | REF615_IED005 - Disturbance Handling | **RED615_IED002 - Parameter Setting**

Group / Parameter Name	IED Value	PC Value	Unit	Min	Max
TOFGAPC1: 1					
TOF(1)					
Off delay time 1	10	**10**	ms	0	3600000
Off delay time 2	0	**0**	ms	0	3600000
Off delay time 3	0	0	ms	0	3600000
Off delay time 4	0	0	ms	0	3600000
Off delay time 5	0	0	ms	0	3600000
Off delay time 6	0	0	ms	0	3600000
Off delay time 7	0	0	ms	0	3600000
Off delay time 8	0	0	ms	0	3600000

TOFGAPC1 function delay explanations:

Off delay time 1: 10ms = The delay between the trip command from differential relay A2 and the closing command to disconnector D_B from relay A2. Note that the trip pulse time of differential relays (20ms) is added to off delay time, i.e., the close command to D_B should thus be given 30ms after the trip pulse from differential relays.

Off delay time 2: 0ms = The delay between the trip command from differential relay A2 and the closing command to circuit breaker CB_DG. Note that the trip pulse time of differential relays (20ms) is added to off delay time, i.e., the close command to CB_DG should be given 20ms after the trip pulse from differential relays. Note that the actual moment at which CB_DG is closed depends on the synchronism check function in the DG relay.

References

[1] O. Rintamäki and J. Ylinen, ”Communicating line differential protection for urban distribution networks”, CIRED 2008, June 2008

[2] Rintamäki, O and Kauhaniemi, K., ”Applying modern communication to loss-of-mains protection”, CIRED 2009, June 2009

[3] Gevean kuormaerottimet ilmajohtoverkkoon, available: http://www.eurolaite.fi/file/kuormaerotin.pdf

[4] Ensto Auguste, SF6-eristetty ilmajohtojen kuormaerotin, available: http://www.ensto.com/download/23601_auguste_fi_lr.pdf

[5] Sähköliittymien suunnitteluohjeet, Vantaan Energia, 26.11.2010, available at: http://www.vantaanenergia.fi/fi/Sahko/SahkoverkotVantaalla/Documents/Tahdistusehdot%20ja%20suojareleiden%20asetteluohje.pdf

[6] Tahdistusehdot ja suojareleiden asetteluohje, E. ON Kainuun Sähköverkko Oy, July 2010, available at: http://www.eon.fi/SiteCollectionDocuments/Tahdistustiedot-ja-suojareleiden-asetteluohje.pdf

[7] Tahdistusohjeet ja suojareleiden asetteluohje, Helen Sähköverkko Oy, 1.1.2009, available at: http://www.helen.fi/urakoitsijat/urakointiohjeet/SU40309L2.pdf

[8] Technical data sheet of medium voltage vacuum power circuit breakers, available at: http://www05.abb.com/global/scot/scot235.nsf/veritydisplay/2221a179df6b9fcf85256d440045001c/$file/ib%206-2-7-7-3i%20vhk%20model%2020_21.pdf

[9] O. Raipala, Real time simulation of active distribution network, M.Sc. thesis, Tampere University of Technology, December 2009

[10] O. Raipala, A. S. Mäkinen, S. Repo, P. Järventausta, ”Interaction of fault ride through requirements and loss of mains protection”, Renewable Energy and Power Quality Journal, No. 11, March 2013

[11] A.G.G. Rodriguez, “Improvement of a fixed speed wind turbine soft−starter based on a sliding mode controller”, Thesis Department of Electrical Engineering, Seville.